Water Dynamics Simulation as a Tool for Probing Proton Transfer Pathways in a Heptahelical Membrane Protein

Christian Kandt, Klaus Gerwert,* and Jürgen Schlitter*
Lehrstuhl für Biophysik, Ruhr-Universität Bochum, Bochum, Germany

ABSTRACT **The proton transfer pathway in a heptahelical membrane protein, the light-driven proton pump bacteriorhodopsin (BR), is probed by a combined approach of structural analysis of recent X-ray models and molecular dynamics (MD) simulations that provide the diffusion pathways of internal and external water molecules. Analyzing the hydrogen-bond contact frequencies of the water molecules with protein groups, the complete proton pathway through the protein is probed. Beside the well-known proton binding sites in the protein interior—the protonated Schiff base, Asp85 and Asp96, and the $H_5O_2^+$ complex stabilized by Glu204 and Glu194—the proton release and uptake pathways to the protein surfaces are described in great detail. Further residues were identified, by mutation of which the proposed pathways can be verified. In addition the diffusion pathway of water 502 from Lys216 to Asp96 is shown to cover the positions of the intruding waters 503 and 504 in the N-intermediate. The transiently established water chain in the N-state provides a proton pathway from Asp96 to the Schiff base in the M- to N-transition in a Grotthus-like mechanism, as concluded earlier from time-resolved Fourier transform infrared experiments [le Coutre et al., Proc Nat Acad Sci USA 1995;92:4962–4966]. Proteins 2005;58:528–537.**

Key words: bacteriorhodopsin; N-intermediate; molecular dynamics simulation; water density; retinal protein; proton pump; internal water; H-bonded network

INTRODUCTION

Proton transfer reactions play a central role in many enzymatic reactions. The light-driven proton pump bacteriorhodopsin (BR) is structurally and functionally well characterized. This provides now the unique opportunity to resolve the proton transfer pathway at atomic resolution in a heptahelical membrane protein (see review[1]). BR-proteins are arranged in trimers forming a two-dimensional (2D) crystalline lattice, the so-called purple membrane, found in *Halobacterium salinarium*. After light excitation, BR's chromophore retinal, which is bound via a protonated Schiff base to Lys 216 of the protein, undergoes an all-*trans* to 13-*cis* isomerization in about 450 fs. Thereby, free energy is stored that drives a photo cycle via the intermediates J, K, L, M, N, and O, characterized by different absorption maxima.[2] During the L to M transition, the central proton binding site, the protonated Schiff base, is deprotonated and its counterion Asp 85 becomes protonated.[3,4] Concomitantly a proton is released from the extracellular surface near Glu204 and Glu194.[5,6] In the M to N reaction, the Schiff base is reprotonated by Asp96.[3] On the cytoplasmic surface, a proton is taken up, which reprotonates Asp96 in the N to O transition.[7] With the final step from O to BR, Asp85 is reprotonated. In total, 1 net proton is transferred from the cytoplasma to the extracellular medium, resulting in a pH gradient over the membrane.

Besides the localized proton binding sites, the Schiff base, Asp85, and Asp96, internal water molecules seem to provide additional delocalized proton binding sites. Protonated water chains cause broad IR continuum bands.[8,9] Absorbance changes of such IR continuums were identified during BR's photo cycle, indicating the deprotonation of protonated water clusters.[6,10] It was concluded that the proton release group to the extracellular medium constitutes an $H_5O_2^+$ or larger protonated water cluster stabilized by Glu204 and Glu194.[6,11,12] High-resolution X-ray structural models support these proposals by resolving several internal water molecules on the release side.[13–15]

Since publication of the first atomic structural models,[16,17] computer simulation has contributed to improve structures and to place waters into cavities left by internal residues. From neutron scattering data, one could initially derive the existence of 4 waters near the Schiff base,[18] and later a total of at least 9 functional waters.[19] Five waters were inserted in the simulation models of Nagel et al.[20] Roux et al.[21] used free energy perturbation to position 4 waters between the Schiff base and Asp96. The later published highly resolved X-ray structures[13,14,22,23] contain at most 2 waters in this region; unequivocal positions of additional water could not be detected here.[22] The present structural models of the ground state contain up to 9 internal water molecules; a combination reveals 10 positions where water is present with high probability. By simulations, Baudry et al.[24] confirmed the existence of the

Grant sponsor: Deutsche Forschungsgemeinschaft; Grant numbers: SFB 480-C3 and GE 599/11-1.

*Correspondence to: Jurgen Schlitter/Klaus Gerwert, Lehrstuhl für Biophysik, Ruhr-Universität Bochum, ND 04, 44780 Bochum, Germany. E-mail: juergen@bph.rub.de and gerwert@bph.rub.de

Received 6 April 2004; Accepted 26 August 2004

Published online 17 December 2004 in Wiley InterScience (www.interscience.wiley.com). DOI: 10.1002/prot.20343

mentioned 4 and 1 additional water, which is hydrogen-bonded to the Schiff base. On the extracellular side, 2 more waters remained near Arg82 during the simulation, which means a total of 7 internal waters. Indications for a water rearrangement after retinal isomerization were found. The simulations have also shown that classical water models are suited to describe internal water except for 1 highly polarized water molecule between the protonated Schiff base and Asp85.[25]

The quality of structures and the available computing time has increased rapidly in the decade after the work of Edholm and Jänig.[26] As a consequence, larger systems are considered and brought closer to equilibrium.[27] They give more reliable insight in the dynamics of all components, which exceeds the information available from structure determination. With particular emphasis on the dynamics of internal and external water, we have recently simulated a BR trimer in explicit membrane water environment at a system size of 84,000 atoms and over 5 ns.[27] This extends the former treatment of Baudry et al.,[24] who simulated monomeric and trimeric BR—the latter in a most natural environment of a fully hydrated membrane patch, but over a much smaller simulation period, which hampers conclusions about the dynamics of internal water.

Mean water densities were computed to describe the anisotropic distribution of internal water molecules. In the protein, 2 large areas of water densities are identified. They are located in the extracellular half of BR containing the waters with the highest dynamics (see Fig. 1). The 8 internal water molecules—as identified by X-ray structure analysis—are organized in the densities entitled IV and V. Density IV consists of the triple water cluster 401BL, 402BL, and 406BL. Note that B and L indicate the authors' initials of the ground state X-ray structural models 1qhj[13] and 1c3w,[14] respectively. Density V is due to water 408B/405L, 403B/407L, 407B, 406B/404L, and 409B. Densities IV and V are intersected by Arg82. In this configuration, they cannot provide a proton pathway in a Grotthus-like mechanism from the Schiff base to the proton release site near Glu204/Glu194 in the ground state. However, we could demonstrate that the arrangement of these 2 water densities seems to be highly sensitive to the conformation of Arg82. By removing the Schiff base charge in a test run, an upward movement of the Arg is induced. After Arg movement, the formerly intersected water densities in the proton release channel merge into one.[27] The orientation of the Arg82 side-chain depends on the protonation state of Asp85, as shown in pK calculations.[11,28,29] X-ray structural models of the M-intermediate (e.g., Sass et al.[15] and Leucke et al.[30]) indicate actually an arginine movement concomitant with protonation of Asp85. IR-investigations also find different orientations during the photo cycle.[31] A movement of Arg82 may establish a direct and continuous Grotthus-like proton pathway from the Schiff base region to the $H_5O_2^+$-complex.[27]

However, it was proposed that the proton is not released directly to the extracellular bulk phase from the $H_5O_2^+$-complex, but other groups on the protein surface must be involved.[6,12] The proton's retention period on the protein surface is pH-dependent: At a pH greater than 5.8, the proton is released to the extracellular bulk phase after 1 ms.[32–35] At a pH smaller than 5.8, this happens not before the O to BR transition.[6] The pathway by which the proton reaches the surface from the $H_5O_2^+$-complex near Glu194/Glu204 is unclear: Is there one single exit funnel, or are several pathways possible due to high side-chain mobility?

Even more unclear is the proton uptake pathway in the cytoplasmic half. The Schiff base is reprotonated by Asp96 in the M- to N-transition.[3] For this to happen, a distance of more than 11 Å needs to be bridged. It is unclear how this

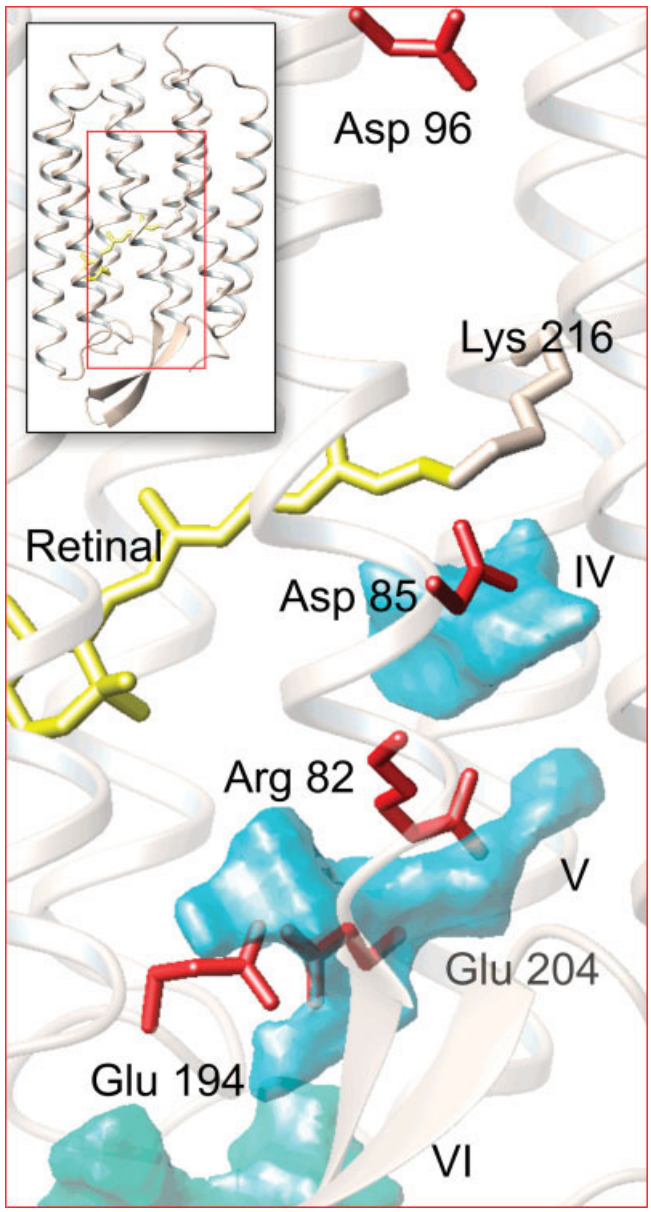

Fig. 1. Display detail of the protein interior. Next to experimentally determined key residues crucial for proton conduction, the mean water densities on the extracellular proton release site are shown. They indicate spatial regions of maximum residence probability for protein internal water molecules. Separated by Arg82, densities IV and V are the largest water densities and contain the waters with the highest dynamics. Density VI is due to temporarily intruding bulk water.

is achieved. There is no water chain observed in the BR structural models in the cytoplasmic half. Either the reprotonation is based on fluctuations of single water molecules and side-chain movements that are not resolved experimentally due to high mobility,[36,37] or further water molecules enter the protein and form a transient conduction chain only established in the M- to N-transition.[4,10,38]

During the N- to O-transition, Asp96 is reprotonated from the cytoplasma. The pathway, however, by which the proton reaches the aspartic acid is not known either. There is no obvious channel for proton movement. On the cytoplasmic surface, Asp38 has been found to be an essential part of the proton translocation pathway, as mutation of this residue slows down the photo cycle.[39] Furthermore, the authors proposed Asp36, Asp102, Asp104, and Glu161 to function as proton collectors.

Obviously, various kinds of experiments did not accomplish a complete description of proton transduction. Simulation methods provide a promising way to fill the gap left by experiments. Here we used the dynamics of the internal water molecules in a molecular dynamics (MD) simulation of a BR trimer embedded in a palmitoyloleoyl-phosphatidylcholine (POPC) membrane and water environment to probe the complete proton pathway in BR. The results are compared to a recent X-ray structural model of the N-intermediate[40] at which the largest conformational change during the photo cycle takes place.

MATERIALS AND METHODS

Simulation Details

The 1.9-Å 1qhj structural model[13] was used for simulation. A cavity analysis via SURFNET[41] was performed, and 2 further water molecules were added. One resembles the position of water 502L of the 1c3w structure, which is not present in the 1qhj entry; the other is sited next to water 501L[14]/404B.[13] The BR trimer was reconstructed, and all missing amino acids (4 N-terminal, 16 C-terminal, 3 incomplete interim) were modeled using Insight II. Under GROMACS, the protein was energy-minimized and short in vacuo MD-runs were performed first to achieve adequate relaxation of the termini toward the main protein, so the protein could be inserted into a 16 × 16 POPC lipid bilayer patch. Details have been described elsewhere.[27] The 16 × 16 lipid patch we used had been built from an equilibrated and fully solvated original 8 × 8 lipid patch provided by Peter Tieleman.[42]

The simulation system comprises of 744 amino acid residues, 391 lipids, and 18,782 water molecules, comprising an overall size of 83,941 atoms. In total, 5 ns of unrestrained classical MD simulation were performed. All calculations were carried out using the GROMACS standard ffgmx force field and the SPC water model.[43,44] The runs were performed on a 10 nodes PIII-450 Linux cluster and a dual-CPU Athlon 1600+.

Apart from Asp96 and Asp115 that were protonated,[3,4] standard protonation states were assumed for all amino acids. To maintain the side-chain conformation of Glu204 and Glu194 in the X-ray structural models, Glu204 was also protonated. Thereby a not explicitly modeled $H_5O_2^+$-complex is regarded as the proton release group.[6,11]

Retinal and Lys216 were treated as one artificial amino acid. For bonded and van der Waals interactions, GROMACS/GROMOS standard parameters were used. Electrostatic interactions were modeled on grounds of QM/MM calculations (BLYP ESP charges) of protonated Schiff base retinal (QM) in the 1c3w bR structural model (MM). These results were kindly provided by Gerald Mathias and Paul Tavan at the Ludwig-Maximilians-University (LMU) Munich (personal communication) and display great similarity to the ones published in Spassov et al.[11] Further details have been given elsewhere.[27]

Water Densities and H-Bond Contact

The expected irregular distribution of water in the protein interior is most easily represented as the distribution in a space-filling rectangular grid.[27,45,46] Our method is essentially analogous to the point frame (PF) method used in Henchman and McCammon.[46] PF-densities are constructed within the absolute reference frame of the complete system and span the whole region defined by water movement. In contrast, time averaged position/averaged residue coordinate (TAP/ARC) water densities[46] are constructed within the relative reference frame of the immediate protein environment. That way a water molecule's location relative to a side-chain can be specified.

The transient structures of all monomers including water molecules are superimposed onto a monomer reference structure. A cubic spatial grid with an edge length of 1 Å connected with the reference structure was used to count the number of water oxygens per subcube and to calculate the mean density as the time-averaged number per $Å^3$. The evaluation was done for 3 ns following the 2-ns equilibration phase. The mean density then is averaged over the 3 monomers.

For visual representation, we considered only voxels exceeding a cutoff density of 0.015 $H_2O/Å^3$, which is ~50% of the value for bulk water under standard conditions. Lower cutoff values result in large and rather undifferentiated distributions, covering regions of low residence probability, whereas higher cutoff levels do not fully regard the water's mobility anymore. Clustering of density voxels was achieved by computing Connolly surfaces for the cells exceeding the cutoff. A probe radius of 1.4 Å was used. Higher cutoff values were used analogously to find the most probable water positions in a density. The use of Connolly surfaces for clustering bears the advantage of having no loss in data, as would be the case when running smoothing operations where each cell represents the average of its own and surrounding neighbor cells' density.

Hydrogen bonds are determined using the GROMACS tool g_hbond with restrictions for the hydrogen donor–acceptor angle (cutoff = 60°) and the hydrogen-acceptor distance (cutoff = 2.5 Å). OH and NH groups are regarded as donors, and O and N as acceptors. The output has the form of time-resolved H-bond trajectories (values 1 or 0) for each pair that at least once is found to form an H-bond.

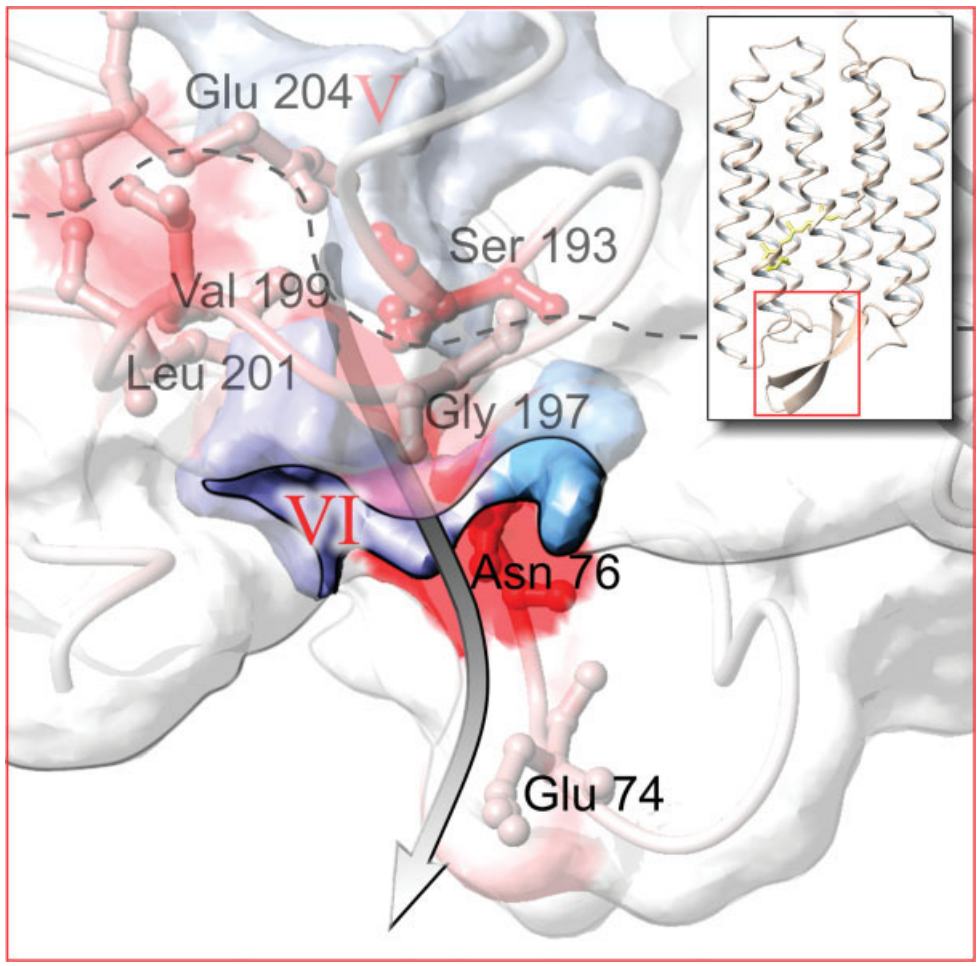

Fig. 2. The identified exit channel by which temporarily associated water molecules can diffuse from the proton release site to the bulk phase. The release site is made up by an $H_5O_2^+$ molecule stabilized by Glu204 and Glu194. The extracellular protein surface is shown in semitransparent side view. The labeled residues of the proton exit pathway are interstations relevant for diffusion. They are colored in shades of red, representing temporal frequency of H-bond contact to water: white, 0%; red, 50%. No water exchange across the dotted line is observed.

The large number of possible partners among 744 amino acids and 18,782 water molecules requires restriction to a selection of interesting groups. As for BR, some functionally important residues are already known, an initial group of key residues was selected. The residues are Thr46, Tyr57, Arg82, Asp85, Asp96, Trp182, Trp189, Ser193, Glu194, Glu204, Ala215, and Lys216. Among them, an influence on proton transfer has been proven experimentally for Arg82, Asp85, Asp96, Glu194, Glu204.[3,4,38] The other residues had been proposed to form H-bonds with water, which is clearly internal in the X-ray models. By a first H-bond analysis where all waters but only the key residues are considered, we identify the subset of "essential" water that interacts with them.

In a second analysis, we monitor the fate of these waters to identify further residues forming H-bond with the water subset. Eventually this yields a complete list of residues that are, at least temporarily, in contact with essential water molecules. For each such residue, the average frequency of H-bond contacts (in percent of simulation time) is determined.

The relatively small number of essential waters allows a classification by visual inspection of trajectories. It was possible to differentiate rather local fluctuations from large-scale, diffusive motions that always mean exchange with the bulk phase. Accordingly we distinguish between permanently internal and temporarily associated water molecules.

Structural Comparison

The 1.62-Å 1p8u X-ray structural BR and N state models[40] were used to compute root-mean-square deviations (RMSDs) per residue via GROMACS tool g_rmsf. Conformational differences were stored as formal B-factors for later visualization in MolMol 2k2.[47] Note that the 1p8u ground state structure is merely identical to the 1.55 Å ground state structure[14]—C_α RMSD = 0.36 Å.

To compare 502L water trajectories from our simulation with experimentally determined water positions the MD-

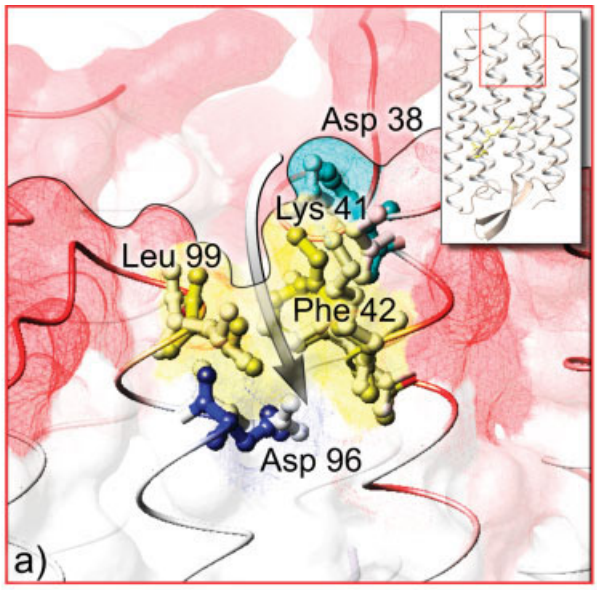

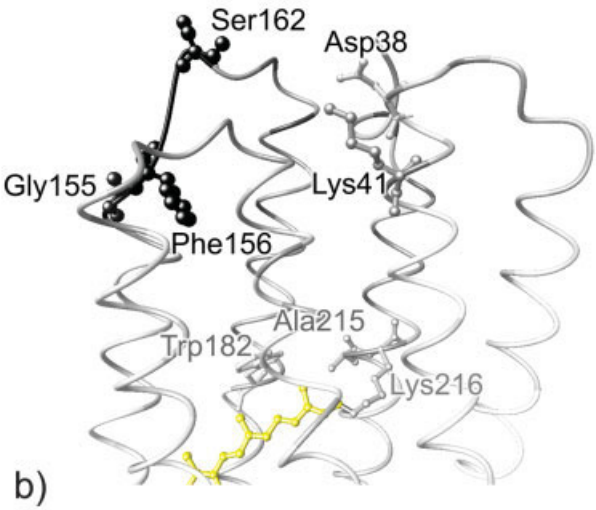

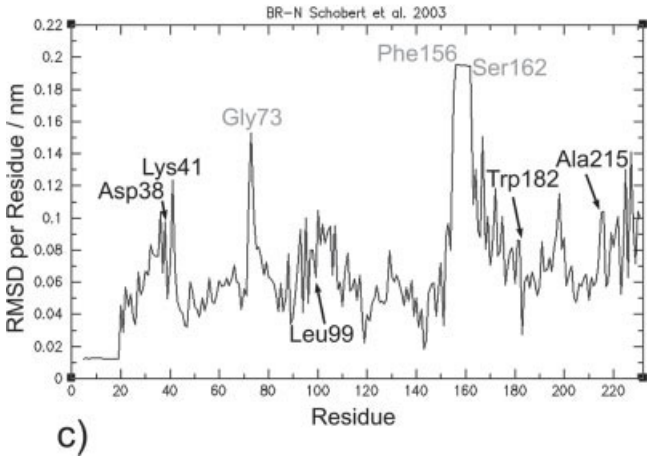

average structure, BR-model 1c3w[14] and N-state model 1p8u[40] were superimposed under MolMol 2k2 taking C_α-atoms of residues 8–152 and 164–230 for reference.

RESULTS AND DISCUSSION

Proton Exit Pathway

Protein internal water molecules are diffusing within 5 spatial regions of high residence probability represented by maxima in the water density. A sixth density at the periplasmic surface is due to intruding bulk waters, which are temporarily associated with the protein, as shown in Figure 2. During the 3-ns observation time, Glu204 and Ser193 form a diffusion threshold between protein internal and temporarily intruding extracellular bulk water, as indicated by the dashed line in Figure 2. Both the mean water densities of the diffusing bulk water molecules and their H-bond frequencies to protein residues are used to probe the possible proton pathway to the extracellular surface.[27] The simulation provides one discrete exit channel, as shown in Figure 2. Glu74, Asn76, Gly197, Val199, and Leu201 are likely to be involved in the proton conduction from the proton release site in density V to the extracellular bulk phase. The finding agrees with the proposal that the $H_5O_2^+$-complex stabilized by Glu194 and Glu204 does not represent the proton release site on the protein surface, but other groups on the surface are involved.[6]

Entry Channel

Also, the H-bond frequencies to bulk water of the cytoplasmic surface of BR were determined [Fig. 3(a)]. As expected, high contact frequency turned out to be a common feature here, and no specific access for cytoplasmic water molecules to the interior of the protein was observed. However, a decreased probe radius—1.0 Å instead of 1.4 Å—for Connolly surface calculation resolves a funnel next to Asp38, Leu99 and Lys41, by which Asp96 becomes accessible for a particle smaller than a water molecule,[27] as shown in Figure 3(a). Leu99 and Lys41 display high H-bond frequency 86% and 100% observation time, respectively. But only Lys41 forms hydrogen bonds via its side-chain. The structural feature of a possible entry funnel was also reported independently.[48] The pathway shown in Figure 3(a) might provide a putative entry channel by which Asp96 could be reprotonated by intruding water due to the conformational change in the M- to N-transition.[7]

As a high resolution X-ray structural model of the N-intermediate is now available,[40] we asked whether one

Fig. 3. Proton uptake channel. Asp96 can be reprotonated from Asp38 by intruding waters when conformational changes later in the photo cycle widen the channel predicted from our calculations. (**a**) Flanking residues are shown both in the average ground state conformation derived from our simulation (colored) and in their N-state conformation (bright) reported by recent X-ray data. A movement of channel residue Lys41 widens the channel. The overall conformational changes between BR ground state and N-intermediate based on recent X-ray models are specified in terms of RMSDs per residue (**b** and **c**). The ground state structural model shown in (b) is color-coded accordingly.

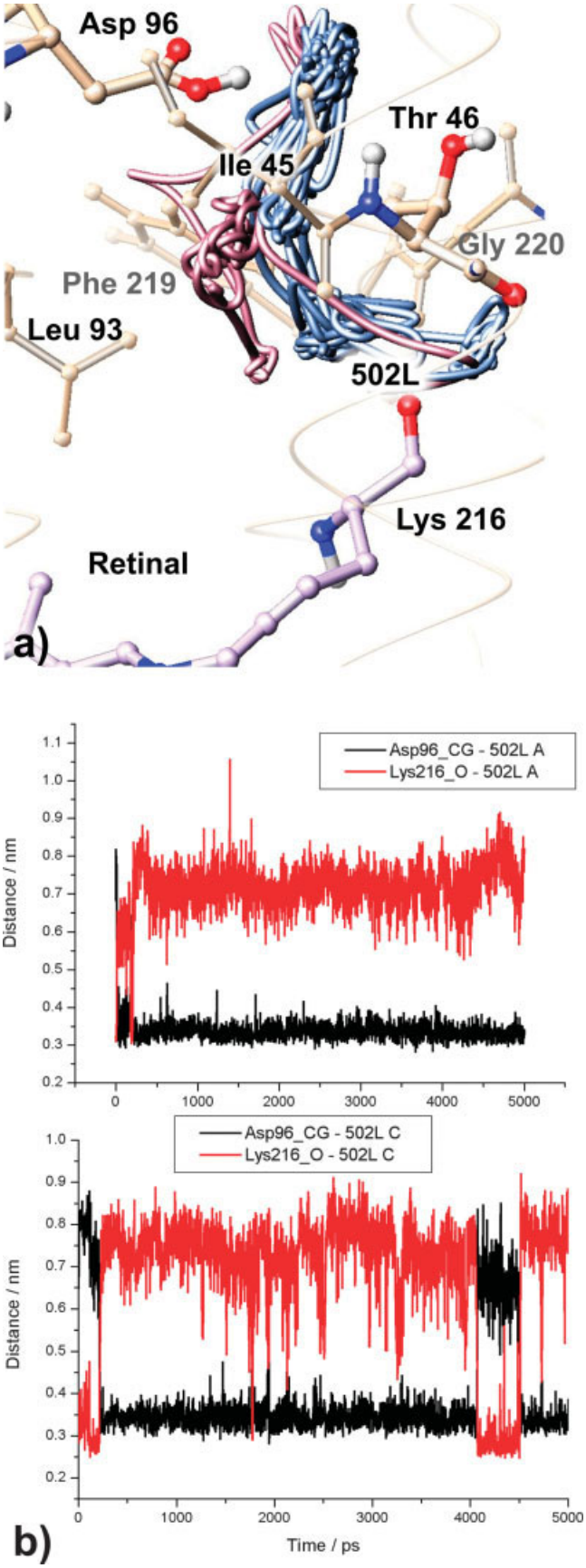

of the identified residues flanking the entry channel exhibits any conformational changes supporting the proposal of an opening of the reprotonation funnel. The structural models of the BR and N-intermediate were compared by computing RMSDs per residue.

RMSDs per residue are shown in Figure 3(b and c). Largest changes are seen in the loop at Gly155, Phe156, and Ser162 (RMSDs: 1.6 Å and 1.9 Å, respectively) flanking the structurally unresolved gap in the EF loop (see also the 1c3w model[14]). This is known to be a very flexible loop region.[13–15] Gly73, also displaying a large change, is positioned in the periplasmic BC loop (RMSD: 1.5 Å). However, Lys41, one of the postulated funnel residues,[27] for which we predicted conformational changes in the later states of the photo cycle, undergoes the expected conformational change. With an average RMSD of 1.2 Å for the whole residue [Fig. 3(b and c)] and an overall movement of more than 2 Å for the side-chain amino group [Fig. 3(a)], Lys41 seems to be an essential part of the opening entry funnel. In addition the probe radius to enter the funnel can be now increased from 1.0 Å to 1.3 Å. However, in the N-state structural model, the channel is still not wide enough to provide a suitable water pathway to Asp96.

A Pathway Between Asp96 and the Protonated Schiff Base

The Schiff base is reprotonated by Asp96, which is located 11 Å away from the central proton binding site.[3] It is proposed that internal waters are involved in the reprotonation pathway.[3,10] However, in the ground state structural models, no such water chain has been identified.

During the simulation time, we observed water 502L leaving its initial position near the backbone of Lys216 and moving close to Asp96.[27] The water's trajectory was analyzed in all 3 monomers. The diffusion of water 502L took place not via an unspecific diffusive movement but via a single pathway in all monomers, as depicted in Figure 4(a). The analysis of distance trajectories between the water oxygen to the Cγ-atom of Asp96 and the peptide O-atom of Lys216 is shown in Figure 4(b). The water movement between Lys216 and Asp96 takes places in both directions: predominantly toward the aspartic acid but also sporadically back again to Lys216. The pathway is flanked by Leu93, Phe219, Gly220, Thr46, and Ile45. The finding points toward a connecting channel between Lys216 and Asp96 by which proton transfer could occur.

How does the proposed pathway fit to the water chain established in the N-intermediate, as recently identified in the X-ray structural model of the N-intermediate?[40] A comparison between the pathway of water 502L in the simulation and the observed N-state water chain is shown

Fig. 4. A connection between Lys216 and Asp96. Shown are the trajectories of water 502L in the framework of the ensemble average structure from simulation (**a**). The graphs indicate the time course of the water's distances to Lys216 (red) and Asp96 (black), respectively (**b**). There is one discrete diffusion pathway where movements take place in both directions.

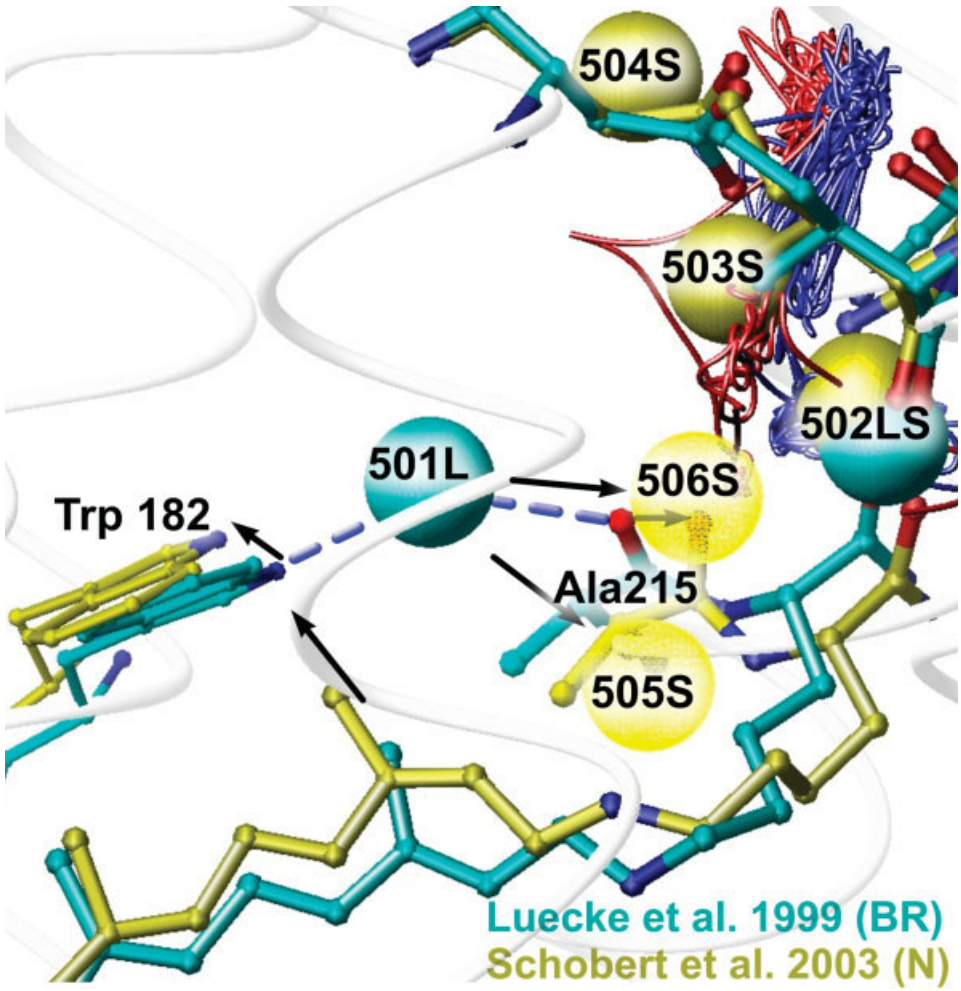

Fig. 5. Overlay of the BR and N structural models together with the positions of internal waters. The positions of N-state waters 502S and 503S coincide with the diffusion pathway predicted by simulation. The arrows represent shifts during the transition from BR to N, which also cause water 501L to move away. Our simulations suggest the presence of 2 waters at the 501L position that later are found as 505S and 506S in the N-intermediate.

in Figure 5. On the cytoplasmic side, there are 2 internal water molecules in the BR ground state (501L, 502L) and 5 in the N-intermediate (502S–506S). Three waters in the N-state are located actually just on the water 502L pathway: 502S and 503S directly, whereas 504S is found close by near Asp96 (Fig. 5). Interestingly, the pathway connecting the Schiff base and Asp96 can obviously be probed by the diffusion of water 502L already in the ground state structural model. The conformational change in the N-state activates this pathway present in the ground state and allows water to intrude.

As a next question, we ask: What protein conformational change established the water chain in the N-intermediate? In the BR ground state water 501L/404B bridges helices F and G via backbone Ala215 and Trp182, as seen in Figure 5.[14,22] The Ala215 backbone can stabilize water 501L because the typical $n - n + 4$ α-helical H-bond pattern is interrupted here. Instead two local $n - n + 5$ hydrogen bonds between Val213 and Gly218, and Ser214 and Phe219 build a structural motif named pi-bulge which in BR was described first in Luecke et al.[14]

In the N-structural model, the C20-methyl group of retinal is moved towards Trp182 due to chromophore isomerization. This induces an upward movement of Trp182 that pushes away water 501L. This disrupts the helix F- and G-bridging hydrogen bonds of water, and Ala215 is no longer stabilized. The backbone carbonyl of Ala215 tilts inward, changing the pi-bulge.

Cavity analysis of the underlying 1qhj BR model detected sufficient space for 1 extra water next to 501L/404B.[27] The 2 water molecules at the 501L/404B position turned out to be stable throughout the 5-ns simulation time, stabilized by the hydrogen bonds to Ala215 and Trp182. These 2 waters proposed at the 501L/404B position in BR are no longer stabilized in the N-state and might shift toward the N-positions 506S and 505S. Consequently, only 2 (504S, 503S) water molecules would have to be assumed to intrude in

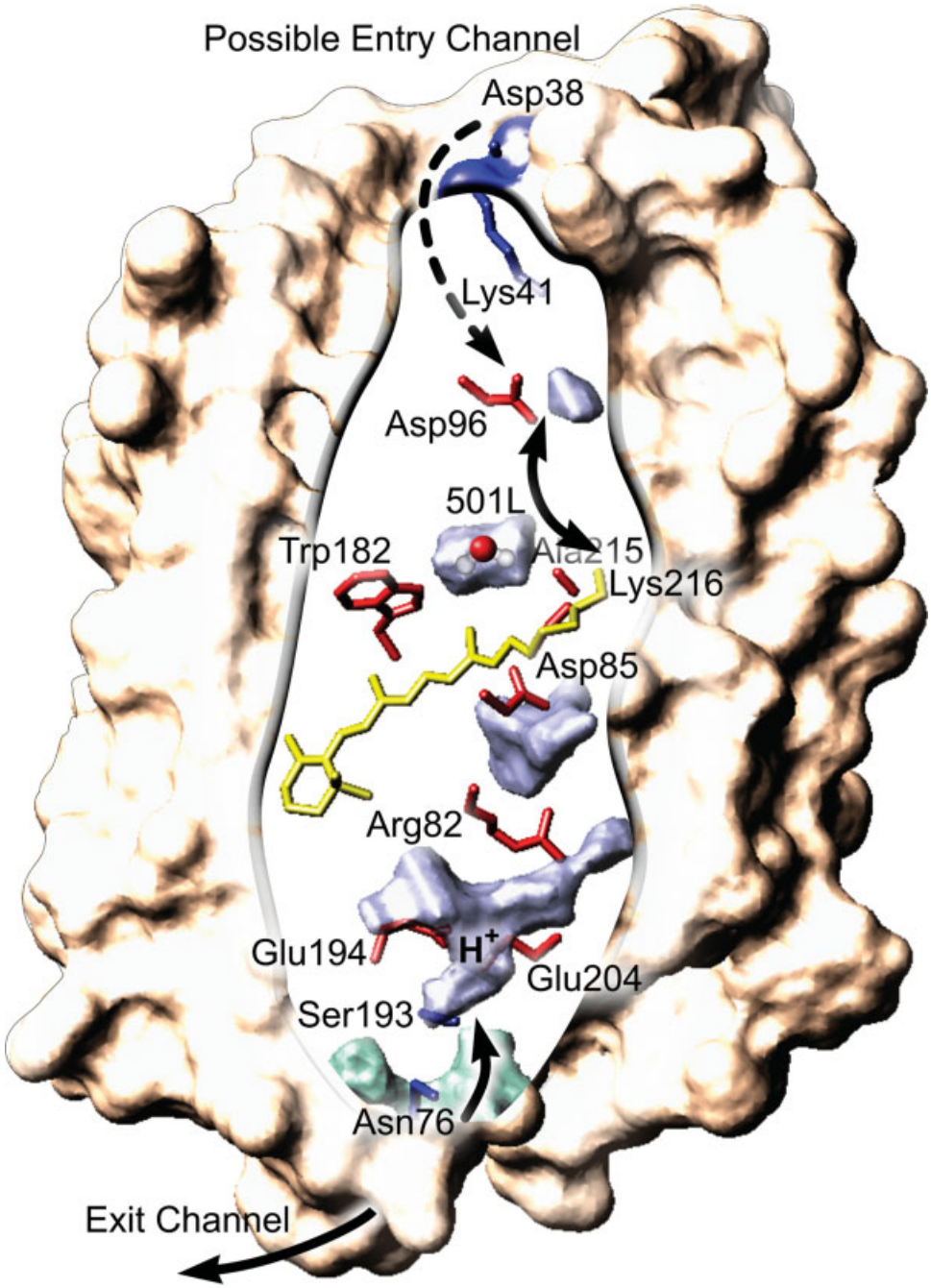

Fig. 6. The complete proton transfer pathway with selected key residues involved. By simulating the diffusion of internal and external water molecules in BR, a plausible complete proton pathway is obtained starting from the ground state structural model.

order to form a water chain leading from Asp96 to the Schiff base. Thereby a transient water chain can be formed during the M- to N-transition without requiring strong water in—and efflux into the proton uptake channel.

CONCLUSIONS

The complete proton pathway in BR is obtained from the ground state structural model by simulating diffusion of internal and external water molecules over a long time and evaluating their distribution on a statistical basis. In comparison with the structural models of the ground and intermediate states, the dynamical behavior provides a more complete picture of water distributions and the participation of many residues in the proton pathway. The agreement with experimental data of the intermediates is astonishing.

For characterizing the cytoplasmic entrance channel, we combined our recent MD simulation[27] of protein and water

with the recently published N-state structural model.[40] The waters probe the pathway from Asp96 to the Schiff base and, at somewhat reduced radius, also the funnel from the surface to Asp96.

In a detailed way, this proceeding explains the delicate movement of water molecules to positions found in N and the concomitant proton conduction in this part of the proton pump. We thus arrive at proposals for two important and not yet fully understood steps of water and protons, from the funnel to Asp96, and from there to the Schiff base. The complete proton pathway derived from the simulation approach is summarized in Figure 6. The theoretical results can be checked now by further biophysical experiments.

ACKNOWLEDGMENTS

We thank Professors Peter Tieleman, Paul Tavan, and Gerald Mathias for their support.

REFERENCES

1. Lanyi JK, Schobert B. Local–global conformational coupling in a heptahelical membrane protein: transport mechanism from crystal structures of the nine states in the bacteriorhodopsin photocycle. Biochemistry 2004;43:3–8.
2. Lozier RH, Bogomolni RA, Stoeckenius W. Bacteriorhodopsin: a light-driven proton pump in *Halobacterium halobium*. Biophys J 1975;15:955–962.
3. Gerwert K, Hess B, Soppa J, Oesterhelt D. Role of aspartate-96 in proton translocation by bacteriorhodopsin. Proc Nat Acad Sci USA 1989;86:4943–4947.
4. Gerwert K, Souvignier G, Hess B. Simultaneous monitoring of light-induced changes in protein side-group protonation, chromophore isomerization, and backbone motion of bacteriorhodopsin by time-resolved Fourier-transform infrared spectroscopy. Proc Nat Acad Sci USA 1990;87:9774–9778.
5. Richter HT, Brown LS, Needleman R, Lanyi JK. A linkage of the pKa's of asp-85 and glu-204 forms part of the reprotonation switch of bacteriorhodopsin. Biochemistry 1996;35:4054–4062.
6. Rammelsberg R, Huhn G, Lubben M, Gerwert K. Bacteriorhodopsins intramolecular proton-release pathway consists of a hydrogen-bonded network. Biochemistry 1998;37:5001–5009.
7. Heßling B, Souvignier G, Gerwert K. A model-independent approach to assigning bacteriorhodopsin's intramolecular reactions to photocycle intermediates. Biophys J 1993;65:1929–1941.
8. Wicke E, Eigen M, Ackermann T. Über den Zustand des Protons (Hydroniumions) in wässriger Lösung. Zeitschrift für Physikalische Chemie (NF) 1954;1:340–364.
9. Zundel G. Proton polarizability and proton transfer processes in hydrogen bonds and cation polarizabilities of other cation bonds: their importance to understand molecular processes in electrochemistry and biology. Trends Phys Chem 1992;3:129–156.
10. Le Coutre J, Tittor J, Oesterhelt D, Gerwert K. Experimental evidence for hydrogen-bonded network proton transfer in bacteriorhodopsin shown by Fourier-transform infrared spectroscopy using azide as catalyst. Proc Nat Acad Sci USA 1995;92:4962–4966.
11. Spassov VZ, Luecke H, Gerwert K, Bashford D. pK(a) calculations suggest storage of an excess proton in a hydrogen-bonded water network in bacteriorhodopsin. J Mol Biol 2001;312:203–219.
12. Garczarek F, Wang J, El-Sayed MA, Gerwert K. The assignment of the different infrared continuum absorbance changes observed in the 3000-1800-cm-1 region during the bacteriorhodopsin photocycle. Biophys J 2004;87:2676–2682.
13. Belrhali H, Nollert P, Royant A, Menzel C, Rosenbusch JP, Landau EM, Pebay-Peyroula E. Protein, lipid and water organization in bacteriorhodopsin crystals: a molecular view of the purple membrana at 1.9 angstrom resolution. Structure 1999;7:909–917.
14. Luecke H, Schobert B, Richter HT, Cartailler JP, Lanyi JK. Structure of bacteriorhodopsin at 1.55 angstrom resolution. J Mol Biol 1999;291:899–911.
15. Sass HJ, Buldt G, Gessenich R, Hehn D, Neff D, Schlesinger R, Berendzen J, Ormos P. Structural alterations for proton translocation in the M state of wild-type bacteriorhodopsin. Nature 2000;406:649–653.
16. Henderson R, Baldwin JM, Ceska TA, Zemlin F, Beckmann E, Downing KH. Model for the structure of bacteriorhodopsin based on high-resolution electron cryo-microscopy. J Mol Biol 1990;213:539–560.
17. Grigorieff N, Ceska TA, Downing KH, Baldwin JM, Henderson R. Electron-crystallographic refinement of the structure of bacteriorhodopsin. J Mol Biol 1996;259:393–421.
18. Papadopoulos G, Dencher NA, Zaccai G, Büldt G. Water molecules and exchangeable hydrogen ions at the active centre of bacteriorhodopsin localized by neutron diffraction: elements of the proton pathway? J Mol Biol 1990;214:15–19.
19. Papadopoulos G, Hauss T. Determination of water molecules in the proton pathway of bacteriorhodopsin using neutron diffraction data. Eur Biophys J 2003;32:392–401.
20. Nagel J, Edholm O, Berger O, Jänig F. Investigation of the proton release channel of Bacteriorhodopsin in different intermediates of the photo cycle: a molecular dynamics study. Biochemistry 1997;36:2875–2883.
21. Roux B, Nina M, Regis P, Smith JC. Thermodynamic stability of water molecules in the Bacteriorhodopsin proton channel: a molecular dynamics free energy perturbation study. Biophys J 1996;71:670–681.
22. Pebay-Peyroula E, Rummel G, Rosenbusch JP, Landau EM. X-ray structure of bacteriorhodopsin at 2.5 angstroms from microcrystals grown in lipidic cubic phases. Science 1997;277:1676–1681.
23. Essen L, Siegert R, Lehmann WD, Oesterhelt D. Lipid patches in membrane protein oligomers: crystal structure of the bacteriorhodopsin–lipid complex. Proc Natl Acad Sci USA 1998;95:11673–11678.
24. Baudry J, Taijkorshid E, Molnar F, Phillips J, K. S. Molecular dynamics study of Bacteriorhodopsin and the purple membrane. J Phys Chem 2001;105:905–918.
25. Hayashi S, Tajkhorshid E, Schulten K. Structural changes during the formation of early intermediates in the bacteriorhodopsin photocycle. Biophys J 2002;83:1281–1297.
26. Edholm O, Jänig F. Molecular dynamics simulation of bacteriorhodopsin. In: Pullman A, Jortner J, and Pullman B, editors. Membrane proteins: structures, interactions and models. Dordrecht: Kluwer Academic; 1992.
27. Kandt C, Schlitter J, Gerwert K. Dynamics of water molecules in the bacteriorhodopsin trimer in explicit lipid/water environment. Biophys J 2004;86:705–717.
28. Bashford D, Gerwert K. Electrostatic calculations of the pKa values of ionizable groups in bacteriorhodopsin. J Mol Biol 1992;224:473–486.
29. Scharnagl C, Fischer SF. Conformational flexibility of arginine-82 as source for the heterogeneous and pH-dependent kinetics of the primary proton transfer step in the bacteriorhodopsin photocycle: an electrostatic model. Chem Phys 1996;212:231–246.
30. Luecke H, Schobert B, Richter HT, Cartailler JP, Lanyi JK. Structural changes in bacteriorhodopsin during ion transport at 2 angstrom resolution. Science 1999;286:255–261.
31. Hutson MS, Alexiev U, Shilov SV, Wise KJ, Braiman MS. Evidence for a perturbation of arginine-82 in the bacteriorhodopsin photocycle from time-resolved infrared spectra. Biochemistry 2000;39:13189–13200.
32. Heberle J, Dencher NA. Surface-bound optical probes monitor protein translocation and surface potential changes during the bacteriorhodopsin photocycle. Proc Nat Acad Sci USA 1992;89:5996–6000.
33. Zimanyi L, Cao Y, Chang M, Ni B, Needleman R, Lanyi JK. The two consecutive M substates in the photocycle of bacteriorhodopsin are affected specifically by the D85N and D96N residue replacements. Photochem Photobiol 1992;56:1049–1055.
34. Heberle J, Riesle J, Thiedemann G, Oesterhelt D, Dencher NA. Proton migration along the membrane surface and retarded surface to bulk transfer. Nature 1994;370:379–382.
35. Alexiev U, Mollaghababa R, Scherrer P, Khorana HG, Heyn M. Rapid long-range proton diffusion along the surface of the purple membrane and delayed proton transfer into the bulk. Proc Natl Acad Sci USA 1995;92:372–376.
36. Dencher NA, Heberle J, Büldt G, Höltje H-D, Höltje M. What do neutrons, X-ray synchrotron radiation, optical pH-indicators, and mutagenesis tell us about the light-driven proton pump bacteriorhodopsin? In: Pullman A, Jortner J, and Pullman B, editors.

Membrane proteins: structures, interactions and models. Dordrecht: Kluwer Academic; 1992. p 69–84.
37. Dencher NA, Heberle J, Büldt G, Höltje H-D, Höltje M. Active and passive proton transfer steps through bacteriorhodopsin are controlled by a light-triggered hydrophobic gate. In: Rigaud JL, editor. Structures and functions of retinal proteins. Vol. 221. John Libbey Eurotext Ltd., Montrouge; 1992. p 213–216.
38. Lanyi JK. Progress toward an explicit mechanistic model for the light-driven pump, bacteriorhodopsin. FEBS Lett 1999;464:103–107.
39. Riesle J, Oesterhelt D, Dencher NA, Heberle J. D38 is an essential part of the proton translocation pathway in bacteriorhodopsin. Biochemistry 1996;35:6635–6643.
40. Schobert B, Brown LS, Lanyi JK. Crystallographic structures of the M and N intermediates of bacteriorhodopsin: assembly of a hydrogen-bonded chain of water molecules between Asp-96 and the retinal Schiff base. J Mol Biol 2003;330:553–570.
41. Laskowski RA. Surfnet—a program for visualizing molecular surfaces, cavities, and intermolecular interactions. J Mol Graphics 1995;13:323–330.
42. Tieleman DP, Sansom MSP, Berendsen HJC. Alamethicin helices in a bilayer and in solution: molecular dynamics simulations. Biophys J 1999;76:40–49.
43. Berendsen HJC, Vanderspoel D, Vandrunen R. Gromacs—a message-passing parallel molecular dynamics implementation. Comput Phys Commun 1995;91:43–56.
44. Lindahl E, Hess B, van der Spoel D. GROMACS 3.0: a package for molecular simulation and trajectory analysis. J Mol Model 2001;7:306–317.
45. Makarov V, Andrews B, Smith P, Pettitt B. Residence times of water molecules in the hydration sites of myoglobin. Biophys J 2000;79:2966–2974.
46. Henchman R, McCammon JA. Extracting hydration sites around proteins from explicit water simulations. J Comput Chem 2002;23:861–869.
47. Koradi R, Billeter M, Wüthrich K. MolMol: a program for display and analysis of macromolecular structures. J Mol Graphics 1996;14:51–55.
48. Schaetzler B, Dencher NA, Tittor J, Oesterhelt D, Yaniv-Checover S, Nachliel E, Gutman M. Subsecond proton-hole propagation in bacteriorhodopsin. Biophys J 2003;84:671–686.